

ULTRAVIOLET SPECTROPHOTOMETRY OF VV CEPHEI¹

Young Woon Kang

Dept. of Earth Science, King Sejong University
Seoul, 133-747, Korea

(Received May 18, 1992; accepted June 1, 1992)

ABSTRACT

The IUE archival spectra of VV Cephei were collected to investigate the eclipse nature in the ultraviolet. The temperature of the B star has been determined, as approximately 30000K, based on the flux distributions during egress. Light curves of VV Cephei were reduced from the spectrophotometry of the IUE archival spectra. Three light curves at the center wavelengths of 2350 Å, 2550 Å and 2850 Å have been analyzed by the modified Wilson and Devinney light curve program. The radii of the B star and M star were deduced to 0.05 and 0.22 of unit separation, respectively. The UV light curves show an evidence that the light was attenuated by the highly opaque atmosphere of the M star.

1. INTRODUCTION

VV Cephei is one of the long period eclipsing binaries with an extended atmosphere. It is very similar to that of Zeta Aurigae stars, excepting the cooler component of VV Cephei being classified as M2 instead of K-type. The first photometric study was made by Gaposchkin (1937) who derived a period of 7430 days. Larsson-Leander (1957, 1959) and Fredrick (1960) confirmed this period. Peery (1966) has computed a new orbital element based on the radial velocity curve. He combined with other orbital elements and found masses of $84 M_{\odot}$ and $41 M_{\odot}$ for M and B stars, respectively.

This system has also been studied astrometrically, but the results have added to rather than solved some of the puzzles. Fredrick (1960) has suggested that astrometric observations show that the parallax is considerably larger than usually accepted, and therefore the primary star may not be a supergiant

The light curve of VV Cephei has been observed primarily by McLaughlin (unpublished) between 1932 and 1957. During and near the eclipse of 1955-57 Larson-leander (1957, 1959) discussed the eclipse data. Fredrick showed two types of variation, one of the long

¹이 연구는 교육부의 1991년도 기초 과학 연구 학술 연구 조성비로 수행된 것임.

period of about 13.7 years and amplitude 0.15 magnitude and the other a shorter period with average time between peaks about 349 days, and amplitude 0.3 magnitude. Peery determined the minimum radii of the M and B type stars are $1620 R_{\odot}$ and $88 R_{\odot}$ assuming an orbital inclination of 90 degrees. For the 1977 eclipse the photometric studies were made by McCook and Guinan (1978), Sato *et al.* (1980), and Huang and Gue (1987).

The end of totality of the 1977 eclipse of VV Cep was predicted to occur in spring 1978 just at the time when IUE Observatory began routine observations. A series of observations with the IUE satellite in the UV spectral region has been carried out to determine the nature of the secondary star and to study the common circumstellar envelope. Hagen *et al.* (1991) described the history of IUE observations for VV Cephei.

In this paper the IUE archived spectra have been collected to investigate the eclipse nature in the UV region. In chapter 2, the continuous spectra between 2000 \AA and 3000 \AA have been analyzed. The temperature of the hotter component were derived from the flux distributions at the egress of VV Cephei. In the third chapter the light curves reduced from the spectrophotometry were analyzed for the size of the hotter component of VV Cephei. The light attenuation is discussed in the last chapter.

2. THE CONTINUOUS SPECTRUM

The low dispersion spectra taken with a large aperture in the long wavelength region were collected in order to measure the continuous fluxes during egress and just after egress of VV Cep. Unfortunately VV Cephei was not observed during totality by the IUE because it was

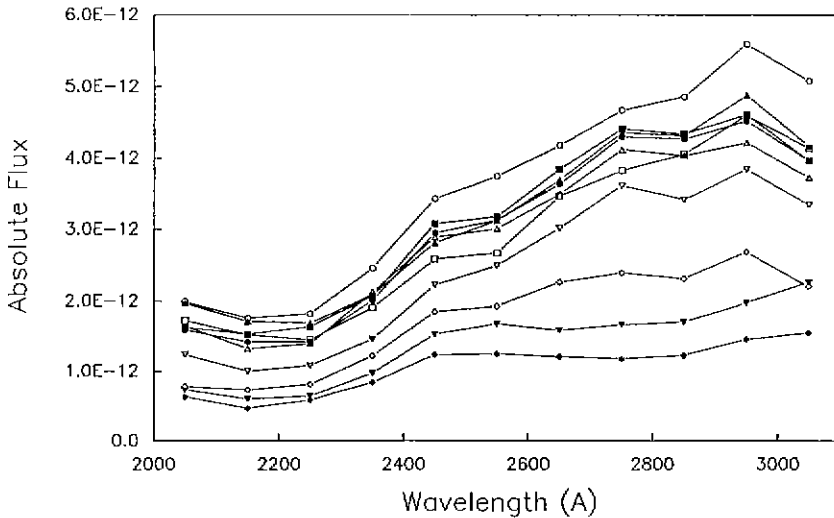


Figure 1. Flux distribution of VV Cephei during egress.

launched after the end of totality. The IUE raw data have been converted to the wavelength versus absolute flux ($\text{erg}/\text{cm}^2/\text{sec}/\text{\AA}$) measured at the earth using the RDAF software of the IUE Observatory. In order to see a variation of the continuous spectra in the region 2000–3000 \AA , the flux ($\text{erg}/\text{cm}^2/\text{sec}/\text{\AA}$) distributions are plotted in Figure 1. The fluxes were averaged at every 100 angstroms from the low dispersion spectra. The orbital phase

Table 1. Mean fluxes of VV Cephei during egress.

Wavelength (\AA)	$0^P.086$	$0^P.083$	$0^P.068$	$0^P.062$	$0^P.056$
2050.0	.199E-11	.159E-11	.165E-11	.197E-11	.173E-11
2150.0	.176E-11	.142E-11	.132E-11	.171E-11	.152E-11
2250.0	.182E-11	.142E-11	.139E-11	.169E-11	.145E-11
2350.0	.246E-11	.201E-11	.213E-11	.209E-11	.191E-11
2450.0	.343E-11	.295E-11	.289E-11	.281E-11	.259E-11
2550.0	.375E-11	.313E-11	.301E-11	.312E-11	.267E-11
2650.0	.418E-11	.364E-11	.350E-11	.370E-11	.347E-11
2750.0	.467E-11	.430E-11	.412E-11	.436E-11	.383E-11
2850.0	.486E-11	.427E-11	.404E-11	.432E-11	.406E-11
2950.0	.559E-11	.452E-11	.422E-11	.488E-11	.460E-11
3050.0	.508E-11	.397E-11	.373E-11	.417E-11	.414E-11

Table 1. (continued)

Wavelengths	$0^P.046$	$0^P.044$	$0^P.043$	$0^P.041$	$0^P.036$
2050.0	.163E-11	.124E-11	.730E-12	.777E-12	.634E-12
2150.0	.153E-11	.100E-11	.602E-12	.729E-12	.466E-12
2250.0	.164E-11	.108E-11	.642E-12	.810E-12	.587E-12
2350.0	.207E-11	.146E-11	.975E-12	.122E-11	.842E-12
2450.0	.308E-11	.223E-11	.153E-11	.185E-11	.124E-11
2550.0	.318E-11	.250E-11	.168E-11	.193E-11	.125E-11
2650.0	.385E-11	.302E-11	.159E-11	.227E-11	.121E-11
2750.0	.441E-11	.362E-11	.167E-11	.240E-11	.118E-11
2850.0	.434E-11	.342E-11	.171E-11	.232E-11	.123E-11
2950.0	.461E-11	.385E-11	.198E-11	.269E-11	.146E-11
3050.0	.397E-11	.335E-11	.227E-11	.221E-11	.155E-11

were calculated using the light element (Wood *et al.* 1980) listed below;

$$\text{Min } I = JD \text{ Hel. } 2435931.4 + 7430^d.5E$$

Table 1 lists the averaged absolute fluxes with orbital phases during egress. The bottom curve in Figure 1 is the flux distribution for the phase 0.03 (just after 3rd contact) where the B star begins to be seen. The top curve is that of the phase 0.083 where the B star is completely out of the eclipse. Other curves in Figure 1 are those for the egress. The spectral gradient is apparently getting steep when the B star is emergent from the eclipse. In order to justify the spectral gradient of the B star during egress, the scale of the flux distribution has been changed from the logarithm scale to the linear scale and the fluxes have been normalized. The normalized flux distribution for each spectrum is plotted in Figure 2. As seen in Figure 2 the shapes of all flux distributions coincide within error bar. Because the B star's light dominates that of the M star at wavelength shorter than 4200 Å, the UV observation is blind for the M star. The flux distribution in UV region provides a good chance for temperature determination of the hotter star. The light change during egress depends only the B star's visible disk area. The mean temperature of emergent flux is not changed during whole phase in UV region. Thus we tried to determine a black-body temperature of the hotter star based on the flux distribution between wavelengths 2000 Å and 3000 Å. A shape of the flux distribution depends on only temperature. Thus we plot theoretical curves for flux distribution of a black-body in Figure 3 to investigate temperature

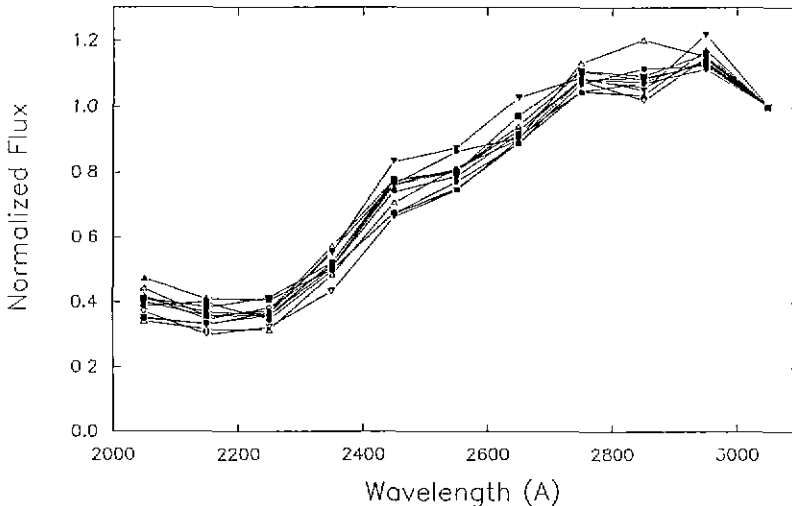


Figure 2. Normalized flux distributions of VV Cephei during egress. Because B star's light dominates that of M star in ultraviolet, the normalized fluxes of VV Cephei during egress show same distribution. All averaged fluxes are normalized to that at the wavelength of 3050 Å.

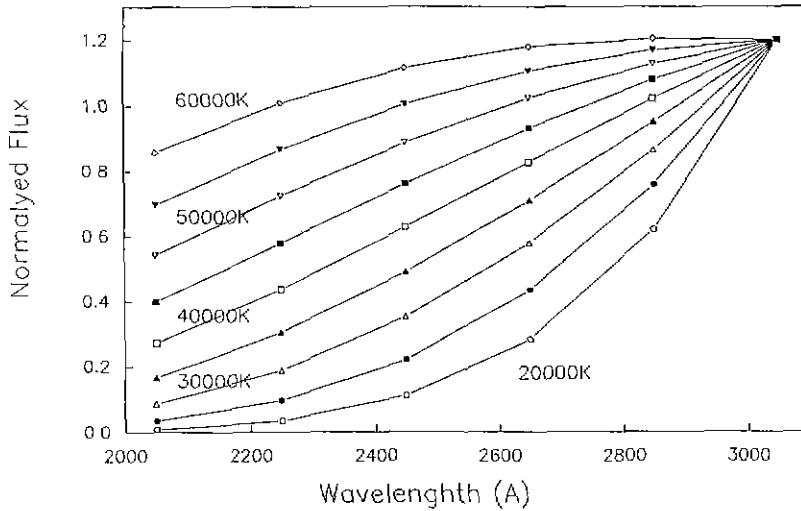


Figure 3. Normalized intensity distributions of a black body. The distribution of the 35000K roughly coincides to that of VV Cephei.

of the hotter star. The theoretical curves were calculated from 20000 K to 60000 K. The best curve fitted to the UV flux distribution of VV Cephei is roughly that of 30000 K which is higher than upper limit of the temperature deduced from its spectral type.

3. LIGHT CURVES FROM SPECTROPHOTOMETRY OF VV CEPHEI

The twenty one IUE spectra of low-dispersion and long wavelength region were reduced for the spectrophotometry of VV Cephei. We integrated the fluxes at the wavelength interval of 100 angstroms for each spectrum (Kang 1990). Thus eleven integrated fluxes between 2000 Å and 3100 Å were reduced for each spectrum. The integrated fluxes were converted to the instrumental magnitudes to construct eleven light curves at the different wavelength regions.

Three among eleven light curves were selected to be analyzed because the three light curves are enough to represent to multi-color curves in the region 2000 Å- 3000 Å. Julian dates, phases and magnitudes for the three light curves are listed in Table 2.

Even if the IUE observations did not cover the whole eclipse, the observations were concentrated during the egress. The phases calculated in chapter 2 have been shifted 0^p.01 to fit to the observations. The UV light curves between phase 0.00 and 0.30 are plotted in

Figure 4. We did not analyze several observations near phase 0.6 in this work. The center wavelengths of the bandpasses for the light curves from top in Figure 4 are 2850 Å, 2550 Å, and 2350 Å. The egress in the UV region lagged behind the visible egress by 2 to 3 months, as a result of higher opacity of the M star atmosphere in the ultraviolet (Hagen *et al.* 1980).

Table 2. UV magnitudes of VV Cephei

JD 240000+	Phase	2350 Å	2550 Å	2850 Å
43649.04000	.0386	6 ^m .3337	6 ^m .5669	6 ^m .3434
43666.56000	.0410	6.0870	5.6564	5.4231
43685.58000	.0436	5.6848	5.1836	5.0393
43689.59000	.0441	5.9279	5.3347	5.0105
43699.98000	.0455	5.4923	4.9073	4.5867
43779.93000	.0563	5.1083	4.6435	4.4027
43821.70000	.0619	5.1993	4.8327	4.3580
43867.72000	.0681	5.1015	4.6644	4.3506
43975.21000	.0825	5.0809	4.7051	4.4718
43975.29000	.0826	5.1422	4.6629	4.4033
44009.19000	.0871	4.9233	4.4653	4.1358
44202.52000	.1131	5.0290	4.5365	4.3000
44253.54000	.1200	5.0160	4.5413	4.3825
44418.78000	.1422	4.9738	4.4983	4.2689
44662.48000	.1750	4.8620	4.3881	4.1054
45010.44000	.2219	4.9718	4.4103	4.1860
47952.35000	.6178	4.9616	4.6800	4.1947
48065.46000	.6330	5.1526	4.4778	4.1056
48414.34000	.6800	5.1644	4.4823	4.1701
48443.98000	.6839	5.3813	4.7583	4.4454
48474.19000	.6880	5.2709	4.5796	4.3193

The fourth contact was occurred at JD 2443748. Although we could not measure the third contact from the UV light curves, the lower limit of a duration between the third and fourth contact is approximately 100 days. In the visible the durations between the third and fourth contact are approximately 30 days for the B star and 87 days for its shell. The duration in UV region is closer to the duration for the B star's shell in visible region. There is no distinction between the B star's emergent and its shell's emergent from eclipse in the UV light curve.

The UV light curves show the light attenuation during 220 days just after fourth contact. As seen in Figure 3, the brightness between the phases $0^P.04$ and $0^P.08$ are $0^m.18$, $0^m.20$ and $0^m.14$ dimmer than those outside eclipse in the light curves of 2350 Å, 2550 Å and 2850 Å,

respectively. The attenuation might be attributed to higher opacity of the M star's extended atmosphere.

VV Cephei is an extremely long period eclipsing binary. The full light curve has not been produced so that the light curve solution was always limited. Our light curves produced from the IUE spectrophotometry cover during and near egress phase, and around phase 0.6.

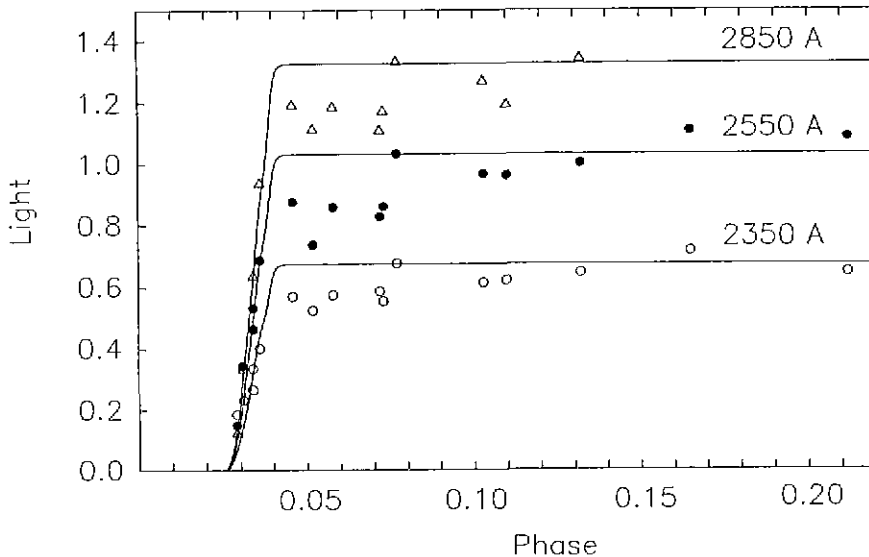


Figure 4. UV light curves of VV Cephei. The symbols are UV observations reduced from the IUE low dispersion spectra and the solid lines are for theoretical light curves. The light between phases 0.04 and 0.07 is dimmer than that outside eclipse.

We concentrated to analyze the egress phase by the Wilson and Devinney (1971, hereafter WD) code for photometric elements. Due to a lack of data it was impossible to find the photometric parameters by the WD differential correction program. The parameters were not conserved by the WD differential correction program for such a small portion of light curve. We modified the Light Curve program of the WD code to calculate lights for three different wavelength regions. Thus instead of the WD differential correction program, the modified WD light curve program was used to find limited solution with trial and error method. The IUE light curves and fitted light curves are plotted in Figure 3 and their parameters are listed in Table 3. In order to fit the slope of the light curve during egress, the radius of the B star should be 0.05 (separation is unit) which is correspond to $350 R_{\odot}$. This radius is much bigger than the radius in optical region estimated to $100 R_{\odot}$ by Perry (1966), but it is corresponding to that of the B stars shell.

4. DISCUSSIONS

The UV light curve of VV Cephei shows somewhat different from the optical light curves. First the egress in visible started earlier than that in ultraviolet. Hagen (1980) also reported that the IUE long-wavelength spectra show the continuum to rise first at the longer wavelengths consistent with the earlier egress in the visible light curves. Our result supports the different egress time between UV and visible, but we don't see any evidence for the different egress time within IUE wavelength region. The temperature of the B star has been reduced without interstellar reddening. Thus it is higher than upper limit deduced from its spectral type. The spectral type of the B star is very uncertain; estimates in the literature range from O8 to A0.

Table 3. Duration, temperature, and radius of VV Cephei in UV region.

Duration between 3rd and 4th contact	100 days
Temperature of B star	30000K
Temperature of M star	3500K
Radius of B star's shell	0.05
Radius of M star	0.22

As seen in Figure 4, the light level at the fourth contact is lower than mean light level outside eclipse and the lower level lasted for 220 days (between the phase 0.042 and 0.073) in the UV light curves. The variation just after 4th contact in ultraviolet is rather jump or erupt than sinusoidal, while the periodic variation was reported in the visible. We can infer that the B star was still affected by the M star's atmosphere even if it was emergent from the eclipse. The atmosphere should be highly opaque in the ultraviolet. We calculated roughly the radius of the atmosphere assuming 90 degree inclination. The radius of the atmosphere is twice of the M star's radius. This does not mean the radius of the M star's whole atmosphere, but the radius of the highly opaque atmosphere in the ultraviolet. Generally light curve gives relatively accurate information about radii of both components. However the radius of the B star shows poor agreement with that in visual. This attributes to the shell of B star. The shell might contribute considerable amount of light as well as the star itself in the UV region.

ACKNOWLEDGEMENTS : I am grateful to the staffs of the KREONET and IUE observatory for archiving the IUE image data. I wish to thank Misses S. H. Choea and J. Y. Kim for editing the manuscript for TeX format and for plotting, respectively. This work was financially supported by the Ministry of Education, Republic of Korea, through

the Natural Science Research Institute, Yonsei University.

REFERENCES

- Fredric, L. 1960, *AJ*, 65, 628.
Gaposchkin, S. 1937, Harvard Circ. No. 421.
Hagen, W., Bauer, W., Stencel, R. & Neff, D. 1991, *ApJS* 90, 175.
Hagen, W., Black, J. & Dupree, A. 1980, *ApJ*, 238, 203.
Huang, Y. & Guo, Z., 1987. *Acta Astrophys. Sinica*, 7, 120.
Kang, Y. W. 1990, *JA&SS*, 7, 57.
Larsson-Leander, G. 1957, *Ark. Astr.* 2, 135.
Larsson-Leander, G. 1959, *Ark. Astr.* 2, 301.
McCook, G. & Guinan, E. 1978, *IBVS* No. 1385.
Peery, B. 1966, *ApJ*, 144, 672.
Sato, M., Saijo, K. & Hayasaka, T. 1980, *PASJ*, 32, 163.
Wilson, R. E. & Devinney, E. J. 1971, *ApJ*, 166, 605.
Wood, F. B., Oliver, J. P., Florkowski, D. R. & Koch, R. H. 1980, *A Finding List for Observers of Interacting Binary Stars* (U. of Pennsylvania press, Philadelphia), p.306.